Separation Science and Technology
Publication details, including instructions for authors and subscription information:
http://www.informaworld.com/smpp/title~content=t713708471

Competitive Adsorption of Basic Dyes onto Calcite in Single and Binary Component Systems

Gülten Atun[a]; Elif Türker Acar[a]
[a] Istanbul University, Faculty of Engineering, Department of Chemistry, Avcılar-Istanbul, Turkey

Online publication date: 15 June 2010

To cite this Article Atun, Gülten and Acar, Elif Türker(2010) 'Competitive Adsorption of Basic Dyes onto Calcite in Single and Binary Component Systems', Separation Science and Technology, 45: 10, 1471 — 1481
To link to this Article: DOI: 10.1080/01496395.2010.485603
URL: http://dx.doi.org/10.1080/01496395.2010.485603

Separation Science and Technology, 45: 1471–1481, 2010

ISSN: 0149-6395 print/1520-5754 online
DOI: 10.1080/01496395.2010.485603

Taylor & Francis
Taylor & Francis Group

Competitive Adsorption of Basic Dyes onto Calcite in Single and Binary Component Systems

Gülten Atun and Elif Türker Acar
Istanbul University, Faculty of Engineering, Department of Chemistry, Avcılar-Istanbul, Turkey

Equilibrium and kinetic behavior of two basic dyes, Methylene Blue (MB) and Safranine T (ST), onto calcite in single and binary component systems have been studied. Experimental equilibrium results have been well predicted by the Freundlich and the Langmuir isotherm models. The model parameters obtained for single solute systems at 298 K have been used for the calculation of adsorption isotherms in binary dye solutions using multi-component isotherm models. Extended Freundlich and extended Langmuir models satisfactorily fit to MB–ST adsorption in binary solutions. A site distribution function which gives information about the affinity of adsorption sites for competing species in a binary system has been mathematically calculated by using Freundlich isotherm parameters. Time-dependent results for single and binary dye solutions have been analyzed according to the Vermeulen and McKay models based on homogeneous and heterogeneous diffusion processes, respectively. Thermodynamic functions for the transition state have been evaluated from the temperature dependence of diffusion coefficients using the Eyring equation.

Keywords adsorption; binary-component system; calcite; methylene blue; safranine T

INTRODUCTION

Adsorption is one of the most efficient techniques of removing dyes from wastewater, especially if the adsorbent is inexpensive and readily available. Locally available geological materials have great interest as inexpensive adsorbents for the purification of organic and inorganic contaminants discharged from various industries. Calcite, which is an abundant calcerous mineral, has attracted recent interest regarding application to adsorption processes of heavy metal ions such as Zn^{2+} (1), Cd^{2+} (2), Pb^{2+} (2,3) and organic pollutants such as aminoalkylphosphonate (4), atrazine (5), benzoic acid (6), malonate (7), pesticides (8), and poly-electrolytes (9). Although calcite has a high adsorption ability for heavy metal ions, no study has been reported which has addressed adsorption of cationic–organic species and dyes. It is well known that geological materials are negatively charged because of isomorphic substitution and extensively used for the removal of cationic dyes. Recently, research has been focused on dye removal from multi-component systems because colored effluents consist of dye mixtures. However, limited data are available in the literature on multi-component dye adsorption because of increased complexity and the increasing number of parameters needed for process description. Multi-component isotherm models have been applied to predict the equilibrium behavior of Toluidine Blue (TB) – CTAB onto clay and sandsone (10), Acid Blue 113 (AB 113) – tartrazine onto fly ash (11), Basic Blue 41 (BB 41) – Basic Red 18 (BR 18) onto activated carbon AC (12), Cibacron Black B – Cibacron Red RB reactive dyes onto sawdust (13), Basic Blue 3 (BB 3) – Basic Red 22 (BR 22), BR 22 – Basic Yellow 21 (BY 21) and BB 3 – BY 21 onto lignite (14), Basic Blue 69 (BB 69) – BR 22, BB 69 – BY 21 and BR 22 – BY 21 onto AC (15), and Basic Red 46 (BR 46) – Basic Yellow 28 (BY 28) onto bentonite (16).

Almost in all the work related to the adsorption kinetics of dyes, the rate constants of the pseudo-first-order and/or pseudo-second-order equations have been determined for single component systems but a few attempts have been made for the calculation of diffusion coefficients to clarify adsorption mechanism. Many single-and two-resistance mass transfer models have been developed by McKay and his co workers (17–23) and solid phase surface diffusion coefficients (D_s) based on homogeneous diffusion as well as external mass transfer (k_f) and intraparticle-or pore-diffusion coefficients (D_p) based on heterogeneous diffusion models have been calculated for some dye adsorbent systems (17–30). However, film diffusion coefficients (D_f) have not been reported in these studies. A limited number of adsorption studies have also been published which consider the effect of varying temperature on the diffusion coefficients (20,24,26–28).

The main objective of this study is to investigate the adsorption performance of calcite as a low-cost adsorbent for the removal of basic dyes from single and binary solutions. Methylene Blue (MB) and Safranin T (ST) which are extensively used basic dyes for comparison of adsorption

Received 24 September 2009; accepted 5 April 2010.
Address correspondence to Gülten Atun, Istanbul University, Department of Chemistry, Faculty of Engineering, Avcılar-Istanbul, 34320 Turkey. E-mail: gultena@istanbul.edu.tr

properties of geological materials have been chosen as probe molecules (31–35). Adsorption equilibria of the dyes in a binary system have been predicted by applying Freundlich and Langmuir isotherm models as well as their extended forms. Freundlich isotherm parameters have been used for the estimation of a site distribution function which gives information about surface heterogeneity having different affinity for competing ions in binary dye solutions. Film-, solid phase surface- and intra-particle diffusion coefficients have been evaluated by applying single and two-resistance diffusion models. The effect of temperature on the diffusion coefficients has been studied to clarify adsorption mechanisms.

EXPERIMENTAL

Adsorbent Specifications

Calcite mineral used as an adsorbent in this study has been collected from Edremit–Kozak deposits in the North Aegean region of Turkey.

The chemical composition of the calcite sample determined from X-ray fluorescence (XRF) analysis is as follows (in %w/w): CaO, 86.99%; Fe_2O_3, 8.06%; SiO_2, 3.06%; K_2O, 0.74%; P_2O_5, 0.64; Al_2O_3, 0.22%; SO_3, 0.17%; SrO 0.11%. X-ray-diffraction (XRD) analysis also show that mineralogical composition calcite content is higher than 85% and hematite, quartz, and, Ca-montmorillonite have been identified as impurities.

The density, BET surface area, and cation exchange capacity of the calcite sample are 2.7 g cm^{-3}, 15 m^2 g^{-1}, and 0.2 meq g^{-1}, respectively. Particle size fraction used in adsorption experiments was in 0.040–0.070 mm range.

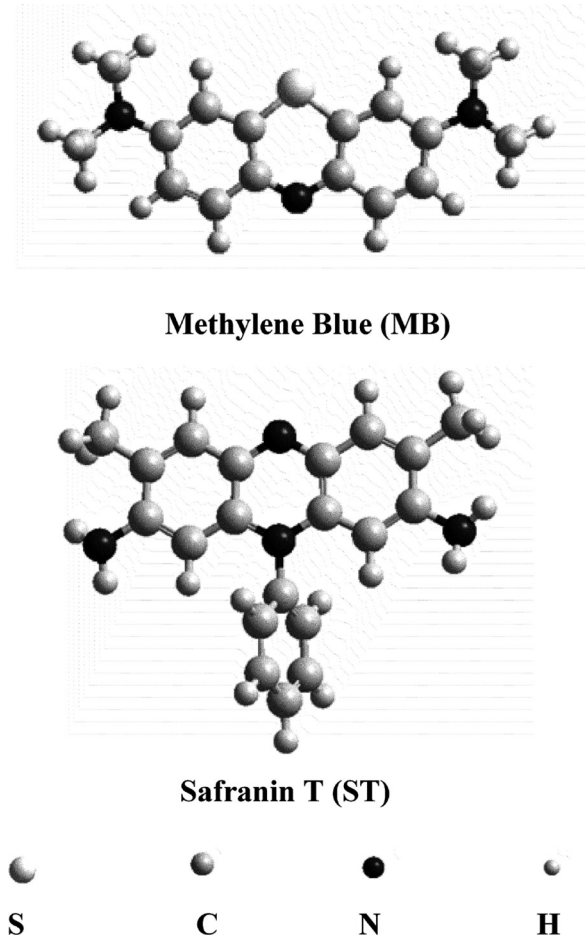

FIG. 1. Chemical structure of the basic dyes.

Adsorbate Specifications

Two basic dye stuffs Methylene Blue (Basic Blue 9) and Safranin T (Basic Red 2) were used in this study. MB is a thio-azine dye ($C_{16}H_{18}N_3SCl$, 3,7-Bis(dimethylamino)-phenazathionium chloride) and ST is a di-azine dye ($C_{20}H_{19}N_4Cl$, 3,7-diamino-2,8 dimethyl-5-phenyl-phenazinium chloride). Their molecular weights are 319.85 and 350.80 g mol^{-1}, respectively. The dyes were supplied from the British Drug Houses Ltd. (purity, 99%) and Sigma Co. (purity, 90%) and, they were used as received. The structural formulas of the dyes drawn using Hyper Chem 8.0 package program were presented in Fig. 1. Dipole moments of MB and ST have been calculated as 2.37 and 3.93 D, respectively.

The concentration of the solutions was determined from UV-vis spectra recorded with Shimadzu 1800 UV-spectrophotometer. UV-vis spectrum of the MB in single dye solutions has a main peak located at 663.5 nm wave length with a shoulder at 618.5 nm. On the other hand, the spectrum of the ST has a maximum at 519.5 nm. The peaks of two dyes are well separated in binary solutions and they can be used for concentration measurements. Dye concentrations in single and binary solutions were determined from the absorbance (A) of the monomer peaks of MB and ST located 663.5 and 519.5 nm, respectively. Calibration plots constructed A vs. dye concentration (C) gave a good linearity according to Beer's Law for $A < 2$. Concentration measurements were made after suitable dilution to follow monomer peaks of dyes. Analytical parameters for the calibration curves, extinction coefficient (ε), limit of detection (LOD) and root mean square error (RMSE), were presented in Table 1.

Adsorption Experiments

Kinetic Studies

Previous experiments showed that an initial dye concentration of 0.5 mM at a solution/adsorbent ratio of 0.051 g^{-1} was suitable for kinetic experiments because equilibrium concentrations were below limit of detection for lower initial concentrations. On the other hand, more dilution was required especially at an earlier time of the adsorption process at higher initial concentrations which

TABLE 1
Analytical parameters for calibration graphs of MB and ST in single and binary solutions

	$\varepsilon \times 10^{-4}$ $1\,mol^{-1}\,cm^{-1}$	LOD $mol\,l^{-1}$	RMSE	r^2
Single				
MB	4.00	7.04×10^{-7}	0.0247	0.9942
ST	3.75	3.10×10^{-8}	0.0025	0.9997
Binary				
MB	3.70	1.47×10^{-7}	0.0136	0.9977
ST	4.19	1.89×10^{-8}	0.0010	0.9997

may be lead to some experimental errors. Time-dependent experiments were carried out by means of the batch method at the temperatures of 298, 208, and 318 K. For each individual test, 0.1 g of adsorbent (accuracy, ±0.0005 g) was placed into screw-capped polypropylene vials of 20 cm^3. A number of vials containing 5 cm^3 of dye solution were agitated in a thermostatic shaker at 200 rpm for 1, 2, 3, 4, 5, 15, 30, and 60 minutes at constant temperature with a precision ±0.01°C. Two phases were separated by centrifugation at 7000 rpm and concentration of the solutions was determined.

Adsorbed fraction (F_t) of solute at any time was calculated from the concentration changes during the adsorption process as follows:

$$F_t = \frac{C_0 - C_t}{C_0} \tag{1}$$

where, C_0 and C_t are solute concentrations (in mmol l^{-1}) at initial and time t, respectively.

Equilibrium Studies

Equilibrium experiments in single and binary component systems were carried out in 0.02–1.00 mM dye solutions at 20 g l^{-1} adsorbent dosage at 298 K. The adsorbent dosage was also decreased up to 2 g l^{-1} in 1.00 mM dye solutions to observe plateau region on adsorption isotherms.

The amount of the adsorbed solute at equilibrium (q_e) was determined by the following equation;

$$q_e = (C_0 - C_e)\frac{V}{m} \tag{2}$$

where, C_e is solute concentration at equilibrium (in mmol l^{-1}) and V/m is the ratio of the solution to the mass of adsorbent (in 1 g^{-1}).

RESULTS AND DISCUSSION

Application of Kinetic Models

The experimental data for time-dependent MB and ST adsorption in single and binary component systems are represented in Fig. 2(a–d). The kinetic results have been analyzed by applying Vermeulen (36) and McKay (37) models based on single and two-resistance diffusion processes, respectively.

Vermeulen Model

Transport within the solid phase for a spherical particle, assuming symmetry in two directions, is given by:

$$\frac{\partial \overline{C}}{\partial t} = D_s\left(\frac{\partial^2 \overline{C}}{\partial r^2} + \frac{2}{r} \times \frac{\partial \overline{C}}{\partial r}\right) \tag{3}$$

Here, $\overline{C}$ is the solid phase concentration of solute (in mmol l^{-1}) and D_s the solid phase surface diffusion coefficient.

The initial and boundary conditions for solution and solid phases are given as

$$\overline{C}(r) = 0 \text{ for } r > r_0 \text{ and } t = 0 \tag{4}$$

$$\overline{C}(r) = \overline{C} = \text{const. } 0 < r < r_0 \text{ and } t = 0 \tag{5}$$

Typical adsorption kinetics is described in terms of fractional attainment of equilibrium U_t at time t and determined experimentally as follows:

$$U_t = \frac{\overline{C}_t}{\overline{C}_e} \tag{6}$$

where, $\overline{C}_t$ and $\overline{C}_e$ are solid phase concentrations of solute (in mmol l^{-1}) at time t and at equilibrium, respectively. The value of U_t also equals to the q_t/q_e ratio and it can be theoretically calculated by applying the Vermeulen equation given as:

$$U_t = [1 - \exp(-\pi^2 P)]^{0.5} \tag{8}$$

here, $P = \frac{D_s t}{r_0^2}$.

The values of U_t have been computed from Vermeulen equation by minimizing standard deviations between experimental and calculated q_t values according to the following relation:

$$\sigma = \left[\frac{1}{n_e}\sum_{i=1}^{n}(q_{t,\exp} - q_{t,\text{cal}})^2\right]^{0.5} \tag{9}$$

where, n_e is the number of experimental observations.

Solid phase surface diffusion coefficients (D_s) calculated by applying the Vermeulen model are shown in Table 2 together with standard deviations. Theoretically calculated curves based on the Vermeulen model are compared with experimental points in Fig. 2(a–d). The values of D_s for MB and ST in single dye solutions are higher than those

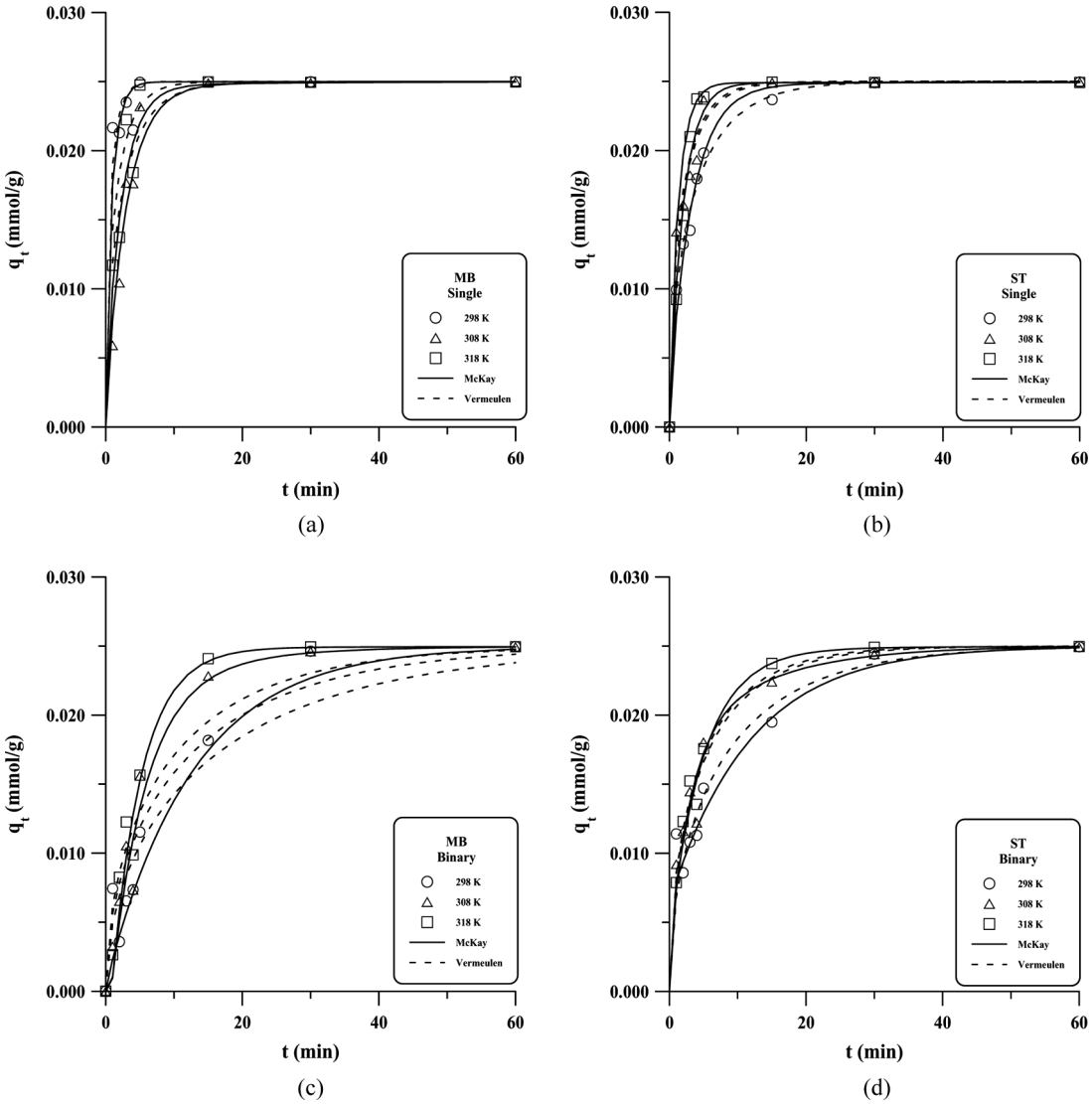

FIG. 2. Time dependency of dye adsorption at different temperatures: (a) MB–, (b) ST in single component systems and, (c) MB–, d) ST in binary component systems. (Solid and dashed lines were estimated according to McKay and Vermeulen models, respectively.).

TABLE 2
Diffusion coefficients calculated from Vermeulen model for MB and ST in single and binary solutions

	Single		Binary	
	MB	ST	MB	ST
T (K)		$D_s \times 10^{13}$ ($m^2 s^{-1}$)		
298	10.96	2.14	0.50	0.98
308	5.04	3.78	0.66	1.49
318	3.28	4.03	0.81	1.59
		σ		
298	0.0019	0.0008	0.0036	0.0021
308	0.0063	0.0012	0.0039	0.0015
318	0.0027	0.0022	0.0036	0.0011

found for their binary systems. The diffusion coefficients increase with the temperature while an inverse effect is observed for MB in its single solution. The increase of D_s values with temperature is consistent with the literature (20,24,26–28). This suggests that solid phase surface diffusion may be a rate-limiting step except for MB in a single-component system.

McKay Model

As can be seen from Fig. 2(a–d), an initial fast stage is followed by a slower process. The McKay equation based on heterogeneous diffusion assumes a film diffusion process corresponding to the initial stage and a particle diffusion process which corresponds to the slower stage. Rate constants k_1 and k_2 corresponding to film- and

particle diffusion processes can be evaluated by analyzing McKay plot (i.e $\ln(1-F_t)=f(t)$ curve). Representative McKay plots are presented in Fig. 3 for MB in a single solute system. These plots have two parts for heterogeneous diffusion processes. The rate of the first section is the sum of the fast and the slow processes. The fast process is completed in an earlier time of adsorption and the second part of the curve corresponds to only the slow process. The rate constant k_2 for the slow process can be calculated from the slope of the second linear portion of McKay plot according to following relation;

$$\ln(1-F_t) = A - k_2(C_t + \overline{C}_t)t \tag{10}$$

In order to obtain the rate constant of the fast process, the final linear portion is extrapolated back to $t=0$ and it is subtracted from the original curve. A straight line is obtained according to the McKay equation in the following form.

$$\ln(1-F_t') = -k_1(C_t + \overline{C}_t)t \tag{11}$$

The values of k_1 can be calculated from the slope of the straight lines given in the inset of Fig 5. Both k_1 and k_2 values (in $1\,mmol^{-1}\,s^{-1}$) for single and binary dye systems are shown in Table 3.

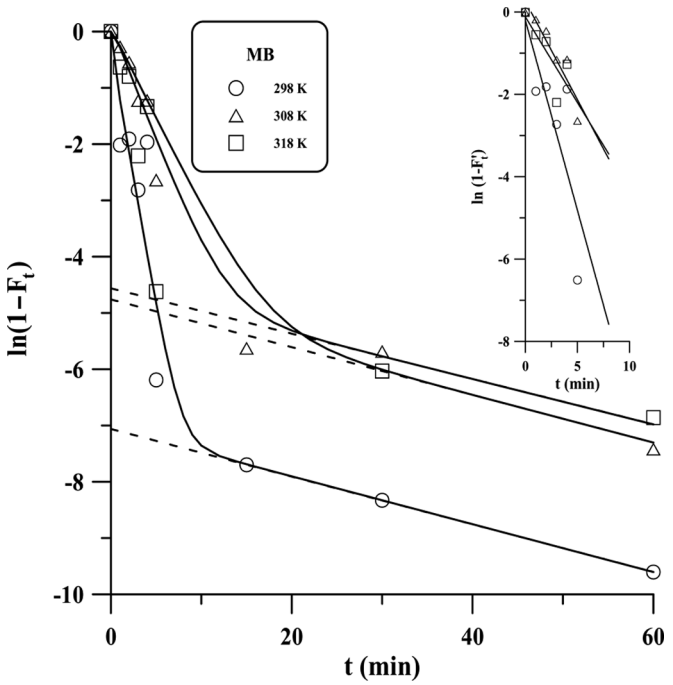

FIG. 3. McKay plots for calculation of rate constants k_2 of the slow process. Inset figure: the plots for calculation of rate constants k_1 of initial fast process. (The curves were modeled using k_1 and k_2 or corresponding diffusion coefficients D_f and D_p, respectively.).

TABLE 3
Kinetic parameters calculated from McKay model for MB and ST in single and binary solutions

	Single		Binary	
	MB	ST	MB	ST
T (K)		$k_1\times10^2$ ($l\,mmol^{-1}\,s^{-1}$)		
298	3.07	0.99	0.27	0.29
308	1.08	1.64	0.66	1.14
318	1.39	2.33	0.75	0.65
		$D_f\times10^{10}$ ($m^2\,s^{-1}$)		
298	7.04	2.28	0.61	0.66
308	2.48	3.76	1.52	2.60
318	3.18	5.35	1.73	1.50
		$k_2\times10^3$ ($l\,mmol^{-1}\,s^{-1}$)		
298	1.42	0.85	2.43	2.70
308	1.41	0.49	2.12	2.60
318	1.34	0.08	0.34	0.90
		$D_p\times10^{14}$ ($m^2\,s^{-1}$)		
298	0.01	0.05	2.25	4.45
308	0.08	0.02	1.56	4.79
318	0.10	0.01	0.01	0.04
		σ		
298	0.0023	0.0011	0.0022	0.0017
308	0.0025	0.0019	0.0024	0.0017
318	0.0024	0.0028	0.0019	0.0013

The film diffusion coefficients D_f (in $m^2\,s^{-1}$) have been evaluated from the k_1 values by using following relation (38,39);

$$D_f = k_1\frac{V\delta\overline{C}_\infty}{A} \tag{12}$$

where, V is the solution volume, δ is the thickness of the liquid film which is assumed equal to mean particle radius, A is the specific surface area of the adsorbent, and $\overline{C}_\infty$ is adsorbate concentration in solid phase determined from the intercept of the extrapolated line in McKay plot. The values of D_f for single and binary dye systems calculated using a film thickness equal to particle radius are presented in Table 3 together with k_1 values.

When particle diffusion contributes on adsorption process following relation can be written similar to the McKay equation (38,39):

$$\ln(1-F_t) = A - \frac{D_p q_1^2}{r_0^2}t \tag{13}$$

where, $A=\ln[6\alpha(\alpha+1)]/(9+9\alpha+\alpha^2q_1^2)$, r_0 is mean radius of particles, q_n's are the non-zero roots of $\tan q_n = (3q_n)/(3+\alpha q_n^2)$ and $\alpha=(3V)/(4\pi r_0^3)$ represents the volume ratio of external solution to the solid particles. Constant k_2 can be correlated to intra-particle diffusion

coefficient (D_p) with a combination of Eqs. (10) and (13) as follows:

$$D_p = k_2 \frac{(C_t + \overline{C}_t) r_0^2}{q_1^2} \tag{14}$$

The values of k_2 and D_p for MB and ST in single and binary component systems are also shown in Table 3. By using the kinetic parameters in Table 3, calculated F_t vs. t curves according to the McKay model are compared to experimental points of MB in single system in Fig. 3. As can be seen from Fig. 2, experimental data for both single and binary component systems are better predicted by two-resistance diffusion model rather than single one.

The magnitudes of film diffusion coefficients for the dyes calculated from McKay model are $\sim 10^{-10}\,m^2\ s^{-1}$ whereas intra-particle diffusion coefficients are nearly 10^3 times lower. On the other hand, D_s values calculated by assuming homogeneous diffusion fall into D_f and D_p values. This suggests that both film and intra-particle diffusion contribute on single solid phase diffusion coefficients. Temperature dependency of D_f and D_s values follows the same direction while D_p values are almost in an opposite direction. This may be arising from higher contribution of D_f on D_s than D_p.

The diffusion coefficients reported in literature have been calculated based on different assumptions and vary in a wide range of 1.1×10^{-16}–$1.8 \times 10^{-9}\,m^2\ s^{-1}$ depending on the adsorbent dosage, particle size, solution concentration, mixing rate, and temperature for various adsorbent–adsorbate systems. Several examples of diffusion coefficients in the literature are as follows: 1.12×10^{-11} and $1.02 \times 10^{-11}\,m^2\ s^{-1}$ for Cibacron Black B and Cibacron Red RB reactive dyes onto sawdust (13); 1.0×10^{-11} and $8.0 \times 10^{-11}\,m^2\ s^{-1}$ for Deorlene Yellow and Telon Blue onto fuller's earth and silica (17); 6.0×10^{-13}, 3.0×10^{-13}, 69 1.1×10^{-12}, 22 $1.0 \times 10^{-12}\,m^2\ s^{-1}$ for AB 25, AR 114, BR 22 and BB 69 onto pith (18,19); $1.2 \times 10^{-13}\,m^2\ s^{-1}$ for BB 69 onto silica (20); 1.5×10^{-13} and $2.1 \times 10^{-13}\,m^2\ s^{-1}$ for AB 25 and BB 69 onto peat (21); 2.0×10^{-13} and $3.0 \times 10^{-14}\,m^2\ s^{-1}$for AB25 and BY 11 onto AC (22); $4.42 \times 10^{-14}\,m^2\ s^{-1}$ and $4.73 \times 10^{-14}\,m^2\ s^{-1}$ for Acid Blue 80 (AB80) and AR 114 onto AC (23); AB 25 onto wood meal ($1.0 \times 10^{-13}\,m^2\ s^{-1}$ (24); 1.81×10^{-9} and $3.18 \times 10^{-13}\,m^2\ s^{-1}$ for Tartrazine onto deoiled soya and bottom ash (25); $1.22 \times 10^{-12}\,m^2\ s^{-1}$ for carminic acid (26); 9.72×10^{-14} and $9.47 \times 10^{-14}\,m^2\ s^{-1}$ for Malachite Green onto AC and slug (27); 2.38×10^{-10} and $2.92 \times 10^{-10}\,m^2\,s^{-1}$ for MB and Methyl Orange (MO) onto AC and slug (28); $(1.84–4.53) \times 10^{-13}$ and $(0.01–54.5) \times 10^{-14}\,m^2\,s^{-1}$ for Acid Red 14 (AR 14) onto AC and hyper-cross-linked polymeric sorbents (29); $(0.58–3.1) \times 10^{-10}$, $(1.3–4.1) \times 10^{-10}$ and $(0.68–2.4) \times 10^{-10}\,m^2\ s^{-1}$ for MB, Basic Blue I (BB I)and AB 74 onto AC (30).

Diffusion coefficients of a solute from solution to the internal phase of the adsorbent follows three steps and decrease in the order of film-, surface-and intra-particle diffusion, respectively. The values of D_f, D_s, and D_p obtained in this study fall into $(0.61–7.04) \times 10^{-10}$, $(0.50–10.96) \times 10^{-13}$, and $(0.01–4.79) \times 10^{-14}\,m^2\ s^{-1}$ range, respectively. These values are comparable with the reported diffusion coefficients in the literature. The increase in the D_p values depending on temperature suggest that MB molecules having smaller size than ST can be diffused up to internal parts of solid phase in single solute system and intra-particle transport is major factors in controlling the rate of adsorption. On the other hand, rate limiting by film and/or surface diffusion process may be more reasonable for larger ST molecules in single solutions as well as for both molecules in binary solutions because of their increasing volumes via solute–solute interactions.

Effect of Temperature on Adsorption Kinetics

Eyring Model

Thermodynamic parameters for transition state can be estimated from the Eyring equation given in following linear form (40):

$$\ln \frac{D}{T} = \text{Ln } 2.72 d^2 \frac{k}{h} + \frac{\Delta S^*}{R} - \frac{\Delta H^*}{T} \tag{15}$$

where, k, h, and R are Boltzmann, Planck, and the universal gas constants, respectively. T is the absolute temperature and d is the average distance between the successive exchanging sites. ΔS^* and ΔH^* are the entropy and the enthalpy of activation, respectively. Their values have been calculated from the intercept and slope of the straight lines in Fig. 4 and presented in Table 4.

The values of Gibbs free energy of activation (ΔG^*) computed using following a well-known equation are also shown in Table 4:

$$\Delta G^* = \Delta H^* - T\Delta S^* \tag{16}$$

Since the values of ΔH^* close to zero Gibbs free energy changes in transition state are entropy controlled. The $\Delta S^* < 0$ and $\Delta G^* > 0$ values show an existence of both entropy and energy barrier in the systems. A negative sign of entropy changes implies that no significant change occurs in the internal structure of the calcite. The energy barrier in activated state may arise partially from hydration of dye cations in the solution phase (38,39). When the ions enter from the solution into the particle surface at least some of the water molecules forming hydration shell of ions are stripped off. Simultaneously, the degree of freedom of ions declines.

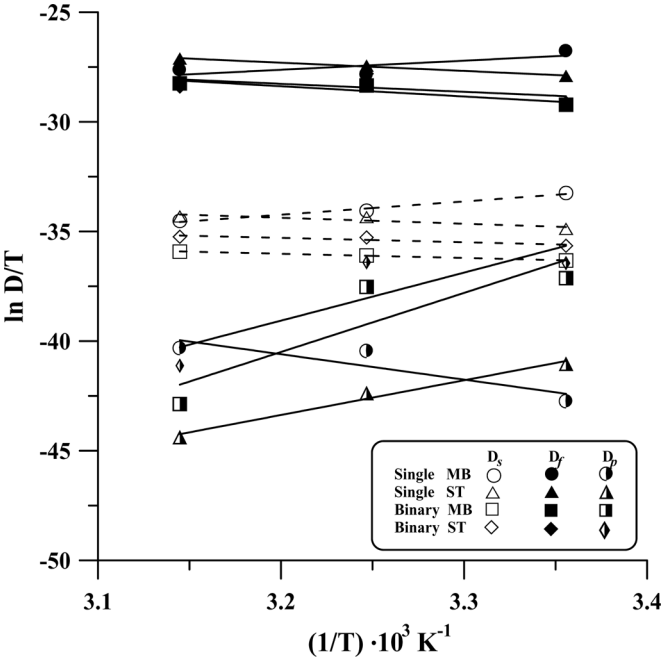

FIG. 4. Eyring plots for calculation of thermodynamic functions at transition state.

Adsorption Equilibria

Dye Adsorption in Single Component Systems

As can be seen from Fig. 5a, adsorption isotherms of MB and ST in single component systems show H shaped curves indicating that calcite mineral has extremely high affinity for both dyes at low concentrations. The dyes are completely removed from the initial concentration range of 0.02–0.04 mM at 20 g l^{-1} adsorbent dosage. A plateau region is observed on the isotherm curves when adsorbent dosage decreases from 20 to 2 g l^{-1} in 1.00 mM dye solutions.

Experimental data have been analyzed by using the Freundlich and Langmuir isotherm equations.

Freundlich Isotherm

The Freundlich adsorption isotherm equation is used for natural adsorbents in which the surface energies are heterogeneous. The equation and its linearized form may be written as follows:

$$q_e = K_F C_e^n \tag{17}$$

$$\ln q_e = \ln K_F + n \ln C_e \tag{18}$$

where, K_F and n are the Freundlich constants related to capacity and surface heterogeneity, respectively. Since the Freundlich equation does not take into account a finite capacity, the values of K_F can be used only comparison purposes of adsorption capacities. Freundlich isotherm parameters for single and binary component systems have been calculated from the slopes and intercepts of the straight lines of ln q_e vs. ln C_e plot in Fig. 6a and presented in Table 5.

Langmuir Isotherm

The Langmuir isotherm equation is another useful model, which assumes a monolayer adsorption on a surface containing a finite number of identical sites. The Langmuir expression and its linear form can be represented as follows:

$$q_e = \frac{K_L q_m C_e}{1 + K_L C_e} \tag{19}$$

TABLE 4
Thermodynamic parameters calculated from Eyring model for transition state of MB and ST in single and binary solutions

				ΔG^* kJ mol^{-1}		
		ΔH^* kJ mol^{-1}	ΔS^* kJ mol^{-1} K^{-1}	298 K	308 K	318 K
D_s	MB single	−0.05	−0.59	176.14	182.05	187.96
	ST single	0.02	−0.36	63.31	65.43	67.56
	MB binary	0.02	−0.39	24.96	25.80	26.64
	ST binary	0.02	−0.39	9.66	9.99	10.31
D_f	MB single	−0.03	−0.49	144.69	149.55	154.40
	ST single	0.03	−0.27	39.54	40.87	42.19
	MB binary	0.04	−0.26	10.21	10.56	10.90
	ST binary	0.03	−0.28	2.93	3.03	3.12
D_p	MB single	0.096	−0.18	52.37	54.12	55.88
	ST single	−0.131	−0.93	48.42	50.04	51.67
	MB binary	−0.224	−1.20	57.87	59.83	61.78
	ST binary	−0.182	−1.05	60.79	62.85	64.91

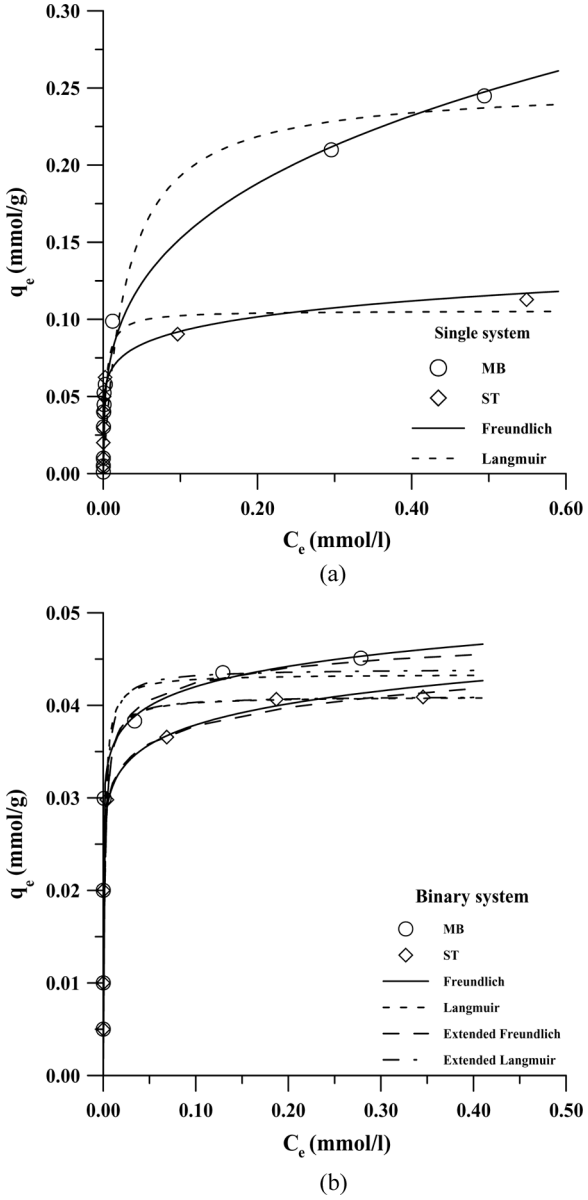

FIG. 5. Adsorption isotherms of MB and ST: (a) in single- (b) in binary dye systems. (Solid lines were estimated according to Freundlich and extended Freundlich models whereas dashed lines were predicted from Langmuir and extended Langmuir models.).

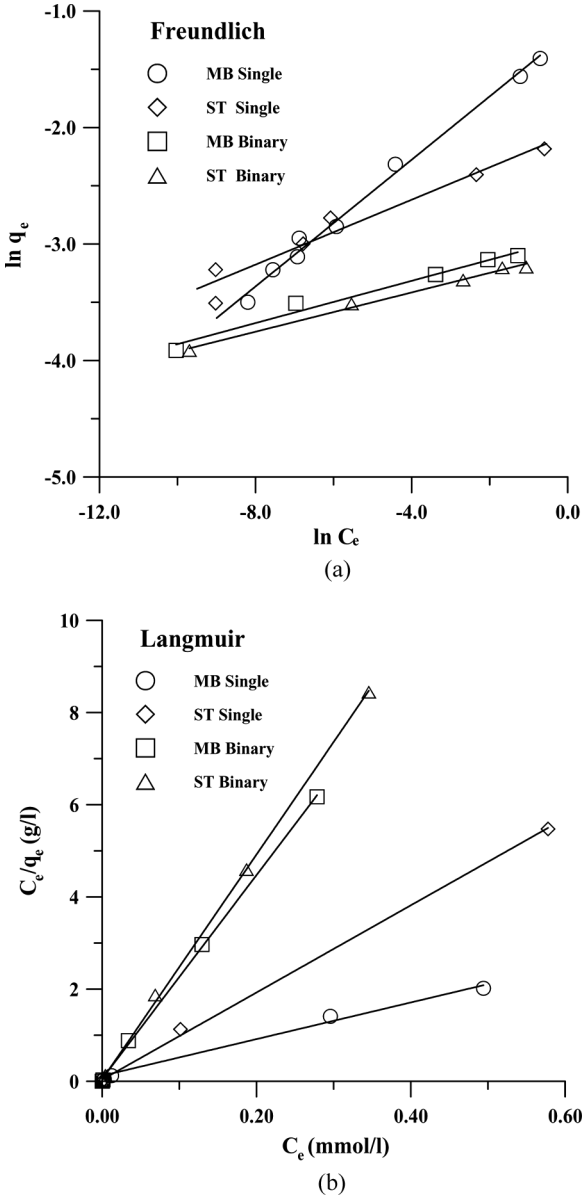

FIG. 6. (a) Freundlich- and (b) Langmuir-adsorption isotherms in linear fashion of MB and ST in single and in binary dye systems.

$$\frac{C_e}{q_e} = \frac{1}{K_L q_m} + \frac{1}{q_m} C_e \tag{20}$$

where, K_L is the Langmuir adsorption equilibrium constant related to the binding energy and q_m is the mono-layer capacity. Langmuir isotherm parameters have been calculated from linear relations from C_e/q_e vs. C_e plots in Fig. 6b and presented in Table 5.

As it is seen from Table 5, the Langmuir adsorption capacities of calcite for MB and ST are 0.252 and

TABLE 5
Freundlich and Langmuir isotherm parameters

	Freundlich			Langmuir		
	n	K_F	r^2	q_m mmol g^{-1}	K_L l mmol^{-1}	r^2
MB Single	0.272	0.305	0.988	0.252	32.9	0.989
ST Single	0.139	0.127	0.948	0.106	262.6	0.999
MB Binary	0.091	0.052	0.980	0.045	394.6	0.999
ST Binary	0.084	0.045	0.993	0.041	576.0	0.999

0.106 mmol g^{-1}, respectively. The lower capacity for ST may arise from structural restrictions because of the phenyl ring bounded to the nitrogen atom of the phenazine ring with right angle. Thus, ST molecules can adsorb only on the external surface sites while MB molecules with smaller size can also access to the internal parts. The reported adsorption capacities of kaolinite, illite, fullers earth, and montmorillonite minerals with different origin for MB are in the range of 0.065–0.072, 0.115–0.270, 0.150–0.396 and 0.770–1.26 mmol g^{-1}, respectively (31–34). Bentonite (i.e., montmorillonite content >85%) also has a high adsorption capacity for ST of 0.767 mmol g^{-1}, (35). The adsorption capacity of calcite for MB is comparable to other clay minerals used for dye removal except for montmorillonite.

Nearly equal monolayer capacities of MB and ST of 0.045 and 0.041 mmol g^{-1} suggest that two dyes are adsorbed together on the adsorbent surface because of solute–solute interactions in binary solutions. This behavior further confirms that the dyes are adsorbed only in external sites on the adsorbent in mixed solutions.

Dye Adsorption in Binary Component Systems

Experimental adsorption equilibrium data for MB and ST in binary solutions are depicted in Fig. 5b. Although H-shaped isotherms are obtained for both dyes competitive adsorption is observed in high concentration region. The values of q_e corresponding to the plateau region are lower than those found for their single isotherms. Equilibrium data for binary dye solutions have been modeled according to following multi-component isotherm equations by minimizing their standard deviations simultaneously between their experimental and calculated values.

Extended Freundlich Model

The amounts of competing components at equilibrium in binary adsorption systems can be calculated using following extended Freundlich isotherm equations (41):

$$q_{e,1} = \frac{K_{F,1} C_{e,1}^{n_1+x_1}}{C_{e,1}^{x_1} + y_1 C_{e,2}^{z_1}} \tag{21}$$

$$q_{e,2} = \frac{K_{F,2} C_{e,2}^{n_2+x_2}}{C_{e,2}^{x_2} + y_2 C_{e,1}^{z_2}} \tag{22}$$

where, $q_{e,1}$ and $q_{e,2}$ are amounts of the first and the second components (i.e., MB and ST) adsorbed at equilibrium; $C_{e,1}$ and $C_{e,2}$ are their remaining concentrations in binary solutions. $K_{F,1}$,and n_1 are individual Freundlich isotherm constants of the first component (MB) in a single solute system as well as $K_{F,2}$,and $n_2$are the parameters of the second component (ST). Other six parameters (x_1, y_1, z_1 and x_2, y_2, z_2) are their extended Freundlich isotherm constants.

TABLE 6
Extended–Freundlich and, –Langmuir isotherm parameters

Extended Freundlich			Extended Langmuir		
	MB	ST		MB	ST
x	−0.282	0.761	q_m (mmol g^{-1})	0.085	
y	5.500	1.850	K (l $mmol^{-1}$)	300	280
z	0.005	0.870			
σ	0.0002	0.0002	σ	0.0121	0.0108

As shown in Fig. 5b, the calculated curves for MB and ST using the extended Freundlich model constants presented in Table 6 are in agreement with the experimental points.

Extended Langmuir Model

The extended Langmuir equation assumes all adsorbate ions or molecules in multi-component systems compete for energetically identical adsorption sites. The amounts of the first and the second components can be calculated as follows (42):

$$q_{e,1} = \frac{q_m K_1 C_{e,1}}{1 + K_1 C_{e,1} + K_2 C_{e,2}} \tag{23}$$

$$q_{e,2} = \frac{q_m K_2 C_{e,2}}{1 + K_1 C_{e,1} + K_2 C_{e,2}} \tag{24}$$

the values of K_1, K_2 and q_m can be calculated from optimized fitting of Eqs. (23) and (24).

The isotherm curves of the MB and ST in binary solutions estimated according to extended Langmuir model are also compared with experimental points presented in Fig. 5b. As can be seen from Fig. 5b and standard deviations presented in Table 6, the extended Freundlich model fit better experimental data than extended Langmuir model.

Site Distribution Function

The Freundlich parameters estimated by assuming a heterogeneous surface have been used in the calculation of a site distribution function of adsorbents in binary solute systems at 298 K. It is assumed that adsorption sites have different affinity for competing ions. They may be grouped into classes, each characterized by the number of sites on the surface and by the relative affinity of surface sites for the adsorbed species. The site distribution function proposed by Sposito is defined as (43):

$$\frac{m_{(q)}}{m_{\max}} = \frac{2\cos(\pi n)\exp[n(q_{\max} - q)] + 2\exp[n(q_{\max} - q)]}{1 + 2\cos(\pi n)\exp[n(q_{\max} - q)] + \exp[2n(q_{\max} - q)]} \tag{25}$$

where, the parameter q represents the class of adsorption sites. $m_q/m_{\max}$ is the ratio of the number of sites of class q to the value of $m_{(q)}$ at its maximum. In order to facilitate calculation of q following relation can be written,

$$q \equiv \ln \frac{K_1}{K_2} \tag{26}$$

Here, K_1 and K_2 are the affinity parameters and $q_{\max}$ is the value of q when $m_q = m_{\max}$. Each of the affinity parameters can be interpreted as relative probability of competing ions to occupy the same adsorption site. Since the Freundlich constant (K_F) is a relative measure of adsorption capacity $q_{\max}$, which is the value of q corresponding to the maximum of site distribution function may be calculated from,

$$q_{\max} = \ln \frac{K_{F_1}}{K_{F_2}} \tag{27}$$

The value of $q_{\max}$ has been estimated as 0.14 using the Freundlich parameters for binary systems presented in Table 5. Using the $q_{\max}$ values and q values chosen arbitrarily its both sides a site distribution functions has been calculated from Eq. (25) and presented in Fig. 7 for the calcite in MB-ST binary system. The function is very similar to a Gaussian curve centered about the $q_{\max}$. The positive region of the curve indicates the surface sites have higher affinity for the first component (i.e., $K_1 > K_2$ and $q > 0$) or vice versa. The positive value of $q_{\max}$ and the slightly lower area under the curves in negative region indicate that the numbers of sites having a higher affinity for MB are greater than for ST. This result is consistent with a slightly higher capacity of MB than ST estimated from the plateau region in Fig. 5b.

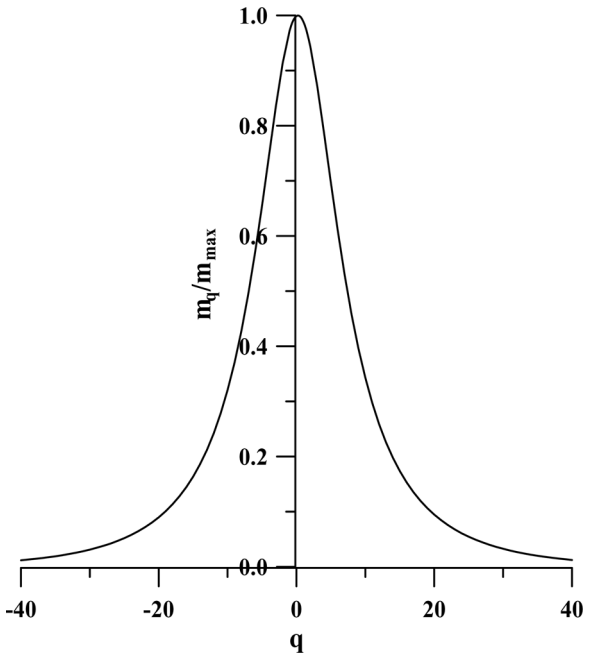

FIG. 7. Site distribution on calcite in MB-ST binary system.

CONCLUSIONS

Kinetic and equilibrium results show that calcite mineral can be successfully used for removal of MB and ST from single and binary dye solutions.

- Film- and particle diffusion coefficients have been calculated from McKay model based on a two-resistance diffusion whereas surface diffusion coefficients have been estimated from the Vermeulen model which assumes homogeneous diffusion process. The magnitude of D_f, D_s, and D_p values decreases in the order $\sim 10^{-10}$, $\sim 10^{-13}$ and $\sim 10^{-14}\,m^2\,s^{-1}$, respectively.
- It has been concluded that intraparticle diffusion is the rate-limiting step for adsorption of MB from a single solution whereas the adsorption of ST is dominated by film and/or surface diffusion processes.
- Thermodynamic parameters calculated from the Eyring model show that both entropy and energy barriers are available in the transition state.
- The H shaped isotherms exhibit that both dyes are completely removed from their individual solutions by calcite in the concentration range of 0.02–0.4 mM at 20 g/l adsorbent dosage.
- The adsorption capacity of calcite for ST is lower than that of MB because of steric effects. The dyes are adsorbed only in external surface sites in binary solutions.
- The site distribution function calculated assuming competitive adsorption show that the number of adsorption sites having higher affinity for MB is slightly greater than for ST.
- Individual Freundlich and Langmuir isotherm parameters for the dyes in single component systems have been used to predict equilibrium behavior of the dyes in binary systems. Extended Freundlich model fits better equilibrium data than extended Langmuir.

The results obtained in this study may be useful for designing a treatment plant for dye removal from single and multi component systems using calcite as a low cost adsorbent.

REFERENCES

1. Shahwan, T.; Zünbül, B.; Tunusoğlu, Ö.; Eroğlu, A.E. (2005) AAS, XRPD, SEM/EDS, and FTIR characterization of Zn^{2+} retention by calcite, calcite–kaolinite, and calcite–clinoptilolite minerals. *J. Colloid Interf. Sci.*, 286: 471.

2. Rouff, A.A.; Reeder, R.J.; Fisher, N.S. (2005) Electrolyte and pH effects on Pb (II)–calcite sorption processes: the role of the $PbCO_3$(aq) complex. *J. Colloid Interf. Sci.*, 286: 61.
3. Chada, V.G.R.; Hausner, D.B.; Strongin, D.R.; Rouff, A.A.; Reeder, R.J. (2005) Divalent Cd and Pb uptake on calcite {10^{-}**1**4} cleavage faces: An XPS and AFM study. *J. Colloid Interf. Sci.*, 288: 350.
4. Kan, A.T.; Fu, G.; Tomson, M.B. (2005) Adsorption and precipitation of an aminoalkyl-phosphonate onto calcite. *J. Colloid Interf. Sci.*, 281: 275.
5. Kovaios, I.D.; Paraskeva, C.A.; Koutsoukos, P.G.; Payatakes, A.C. (2006) Adsorption of atrazine on soils: Model study. *J. Colloid Interf. Sci.*, 299: 88.
6. Madsen, L.; Grøn, C.; Lind, I.; Engell, J. (1998) Adsorption of benzoic acid on synthetic calcite dispersed in cyclohexane as a function of temperature. *J. Colloid Interf. Sci.*, 205: 53.
7. Salinas-Nolasco, M.F.; Méndez-Vivar, J.; Lara, V.H.; Bosch, P. (2004) Passivation of the calcite surface with malonate ion. *J. Colloid Interf. Sci.*, 274: 16.
8. Clausen, L.; Fabricius, I.; Madsen, L. (2001) Adsorption of pesticides onto quartz, calcite, kaolinite, and α-alumina. *J. Environ. Qual.*, 30: 846.
9. Eriksson, R.; Merta, J.; Rosenholm, J.B. (2007) The calcite/water interface I. Surface charge in indifferent electrolyte media and the influence of low-molecular-weight polyelectrolyte. *J. Colloid Interf. Sci.*, 313: 184.
10. Atun, G.; Tunçay, M.; Hisarli, G.; Talman, R.Y.; Hoşgörmez, H. (2009) Adsorption equilibria between dye and surfactant in single and binary systems onto geological materials. *Appl. Clay Sci.*, 45: 254.
11. Pura, S.; Atun, G. (2009) Adsorptive removal of acid blue 113 and tartrazine by fly ash from single and binary dye solutions. *Separ. Sci. Technol.*, 44: 75.
12. Noroozi, B.; Sorial, G.A.; Bahrami, H.; Arami, M. (2008) Adsorption of binary mixtures of cationic dyes. *Dyes Pigments*, 76: 784.
13. Chakraborty, S.; Basu, J.K.; De, S.; Gupta, S.D. (2006) Adsorption of reactive dyes from textile effluent using sawdust as the adsorbent. *Ind. Eng. Chem. Res.*, 45: 4732.
14. Choy, K.K.H.; Allen, S.J.; McKay, G. (2005) Multicomponent equilibrium studies for the adsorption of basic dyes from solution on lignite. *Adsorption*, 11: 255.
15. McKay, G.; Al-Duri, B. (1991) Extended empirical Freundlich isotherm for binary systems: a modified procedure to obtain the correlative constants. *Chem. Eng. Process.*, 29: 133.
16. Turabik, M. (2008) Adsorption of basic dyes from single and binary component systems onto bentonite: Simultaneous analysis of Basic Red 46 and Basic Yellow 28 by first order derivative spectrophotometric analysis method. *J. Hazard. Mater.*, 158: 52.
17. McKay, G.; Otterbrun, M.S.; Aga, J.A. (1987) Pore diffusion and external mass transport during dye adsorption on to fuller's earth and silica. *J. Chem. Techol. Biotecnol.*, 37: 247.
18. McKay, G. (1998) Application of surface diffusion model to the adsorption of dyes on Bagasse Pith. *Adsorption*, 4: 361.
19. McKay, G.; El Geundi, M.S.; Mansour, I.S. (1987) Adsorption of dyes onto bagasse pith using a solid diffusion model. *Water Res.*, 21: 1513.
20. McKay, G.; Allen, S.J. (1984) Pore diffusion model for dye adsorption onto peat in batch adsorbers. *Canadian J. Chem. Eng.*, 62: 340.
21. McKay, G.; Allen, S.J. (1983) Single resistance mass transfer models for adsorption of dyes on peat. *J. Separ. Process. Technol.*, 4: 1.
22. McKay, G. (1984) Two-resistance mass transfer models for the adsorption of dyestuffs from aqueous solutions using activated carbon. *Chem. Tech. Biotechnol.*, 34: 294.
23. Ko, D.C.K.; Porter, J.F.; McKay, G. (2002) A branched pore model analysis for the adsorption of acid dyes on activated carbon. *Adsorption*, 8: 171.
24. McKay, G.; McConvey, I.F. (1985) Adsorption of acid dye onto woodmeal by solid diffusional mass transfer. *Chem. Eng. Process.*, 19: 287.
25. Mittal, A.; Mittal, J.; Kurup, L. (2006) Adsorption isotherms, kinetics and column operations for the removal of hazardous dye, Tartrazine from aqueous solutions using waste materials-Bottom Ash and De-Oiled Soya, as adsorbents. *J. Hazard. Mater. B.*, 136: 567.
26. Atun, G.; Hisarli, G. (2003) Adsorption of carminic acid, a dye onto glass powder. *Chem. Eng. J.*, 95: 241.
27. Gupta, V.K.; Srivastava, S.K.; Mohan, D. (1997) Equilibrium uptake, sorption dynamics, process optimization, and column operations for the removal and recovery of malachite green from wastewater using activated carbon and activated slag. *Ind. Eng. Chem. Res.*, 36: 2207.
28. Singh, K.P.; Mohan, D.; Sinha, S.; Tondon, G.S.; Gosh, D. (2003) Color removal from wastewater using low-cost activated carbon derived from agricultural waste material. *Ind. Eng. Chem. Res.*, 42: 1965.
29. Valderrama, C.; Cortina, J.L.; Farran, A.; Gamisans, X.; de las Heras, F.X. (2008) Kinetic study of acid red "dye" removal by activated carbon and hyper-cross-linked polymeric sorbents Macronet Hypersol MN200 and MN300. *React. Funct. Polym.*, 68: 718.
30. Wu, F.C., Tseng, R.L.; Juang, R.S. (2005) Preparation of highly microporous carbons from fir wood by KOH activation for adsorption of dyes and phenols from water. *Sep. Purif. Technol.*, 47: 10.
31. Atun, G.; Hisarli, G.; Sheldrick, W.S.; Muhler, M. (2003) Adsorptive removal of methylene blue from colored effluents on fuller's earth. *J. Colloid Interf. Sci.*, 261: 32.
32. Kahr, G.; Madsen, F.T. (1995) Determination of the cation exchange capacity and the surface area of bentonite, illite and kaolinite by methylene blue adsorption. *Appl. Clay Sci.*, 9: 327.
33. Ramachandran, V.S.; Kackerand, K.P.; Perwardhan, N.K. (1962) Adsorption of dyes by clay minerals. *Am. Mineral.*, 17: 165.
34. Hang, P.T., Brindley, G.V. (1970) Methylene Blue Adsorption by clay minerals. Determination of surface areas and cation exchange capacities. *Clay and Clay Miner.*, 18: 203.
35. Hu, Q.H.; Qiao, S.Z.; Haghseresht, F.; Wilson, M.A.; Lu, G.Q. (2006) Adsorption study for removal of basic red dye using bentonite. *Ind. Eng. Chem. Res.*, 45: 733.
36. Helfferich, F. (1962). *Ion Exchange*, Chap. 6; Dover: New York.
37. MacKay, H. (1938) Kinetics of isotopic exchange reactions. *Nature*, 142: 997.
38. Huang, T.C.; Tsai, F.N. (1970) Kinetic studies on the isotopic exchange of calcium ion and calcium carbonate. *J. Inorg. Nucl. Chem.*, 32: 17.
39. Huang, T.C.; Li, K.Y.; Hoo, S.C. (1972) Mechanism of isotopic exchange reaction between calcium ion and calcium oxalate. *J. Inorg. Nucl. Chem.*, 34: 47.
40. Wahl, A.C.; Bonner, N.A. (1958). *Radioactivity Applied to Chemistry*; John Wiley and Sons, Inc.: New York.
41. Fritz, W.; Schluender, E.U. (1974) Simultaneous adsorption equilibria of organic solutes in dilute aqueous solutions on activated carbon. *Chem. Eng. Sci.*, 29: 1279.
42. Yang, R.T. (1987) *Gas Separation by Adsorption Processes*; Butterworths: Boston, MA.
43. Sposito, G. (1981) *The Thermodynamics of Soil Solutions*; Clarendon Press: Oxford, UK.